Available online at www.sciencedirect.com
SCIENCE DIRECT®
Journal of Photochemistry and Photobiology A: Chemistry 160 (2003) 69–76
Journal of Photochemistry and Photobiology A:Chemistry
www.elsevier.com/locate/jphotochem

Layer-by-layer accumulation of cadmium sulfide core—silica shell nanoparticles and size-selective photoetching to make adjustable void space between core and shell

Tsukasa Torimoto [a,b], Jocelyn Paz Reyes [a], Shin-ya Murakami [b], Bonamali Pal [b], Bunsho Ohtani [a,*]

[a] *Catalysis Research Center, Hokkaido University, Sapporo 060-0811, Japan*
[b] *Light and Control, PRESTO, Japan Science and Technology Corporation (JST), Japan*

Received 25 December 2002; received in revised form 12 February 2003; accepted 10 April 2003

Abstract

Layer-by-layer accumulation of monolayers of silica-coated cadmium sulfide (CdS) was achieved through repeated monolayer deposition–hydrolysis cycles using CdS particles (average diameter: 5 nm) modified with 3-mercaptopropyltrimethoxysilane (MPTS) and glass substrates. Absorption spectroscopic analyses of the resulting yellow films revealed that each layer had almost the same thickness, the estimated density of which corresponded to ca. 66% of that for close hexagonal packing of nanoparticles. Monochromatic light irradiation at 488, 458, or 436 nm onto the film immersed in oxygen-saturated aqueous methylviologen solution caused a decrease in the size of the CdS core depending on the irradiation wavelength, while atomic force microscopic analyses suggested that the size of the silica shell of the immobilized nanoparticles was almost unchanged by irradiation, i.e., the immobilized silica-coated CdS nanoparticles had void spaces between the photoetched core and the silica shell, and their sizes could be regulated by choosing the wavelength of irradiation light. This size-selective photoetching was applied to nanoparticulate films that had been heat-treated at 473, 573 or 673 K to observe the blue-shift of the absorption edge of CdS to the irradiation wavelength. The amount of CdS remaining in the film after the photoetching process depended on the temperature of heat treatment. The largest amount among as-prepared and heat-treated samples was obtained at 473 K and decreased with an increase in temperature. The growth of particles, i.e., the diminution of particle number, and/or the diminution of number of separated independent shells may account for this dependence.

Keywords: Core–shell structure; Nanoparticles; Void space; Layer-by-layer accumulation; Cadmium sulfide; Photoetching

1. Introduction

Surface coating of nanoparticles with different materials to produce core–shell structures have attracted much attention [1–21] because physical and chemical properties of core materials can be modified or tailored by the shell components with negligible change in shape and size of the core particles. Also, core–shell nanoparticles have been useful as precursors for the preparation of hollow structures by removing core materials through chemical etching or combustion [22–30], and partial removal of the core has enabled preparation of novel nanostructures inside the shell, such as the encapsulation of metal nanoparticles in a hollow sphere and void formation between the core and shell [31–37]. These nanocomposites are an interesting and increasingly important class of materials and have been studied with the aim of developing catalysts, optoelectronic devices and sensors. To utilize these particles in solid devices, it is necessary to immobilize core–shell nanoparticles onto solid substrates. Various techniques for this, including casting of particles [10,38] and the layer-by-layer deposition using charged particles and ionic polymers [39–41], have been reported in recent years.

We have reported a size-selective photoetching technique as a means for preparing monodisperse semiconductor nanoparticles in the size quantization regime. When the technique was applied to CdS, the particle size could be controlled within the range of 3.5–1.7 nm simply by selecting the wavelength of monochromatic irradiation light in the range of 488–365 nm [42–47]. Recently, we have successfully applied this technique to the control of core size in silica-coated CdS nanoparticles, i.e., a CdS core–silica shell structure. The resulting nanoparticles had a void space

* Corresponding author. Tel.: +81-11-706-3673; fax: +81-11-706-4925.
E-mail address: ohtani@cat.hokudai.ac.jp (B. Ohtani).

1010-6030/03/$ – see front matter © 2003 Elsevier Science B.V. All rights reserved.
doi:10.1016/S1010-6030(03)00223-5

inside the silica shell, the size of which could be adjusted by choosing the irradiation wavelength [48]. In this paper, we report a newly developed method of layer-by-layer accumulation of silica-coated CdS nanoparticles on glass substrates. We found that the size of the core, i.e., the size of the void space, in the nanoparticle films could be controlled by using size-selective photoetching.

2. Experimental section

2.1. Materials

Sodium bis(2-ethylhexyl) sulfosuccinate (AOT), 1,1′-dimethyl-4,4′-bipyridinium dichloride (MV^{2+}), and 3-mercaptopropyltrimethoxysilane (MPTS) were purchased from Tokyo Chemical Industry, and cadmium perchlorate was obtained from Kishida Reagents Chemicals. Other chemicals were supplied from Wako Pure Chemical Industries. Aqueous solutions were prepared with purified water just before use by a Yamato/Millipore WP501 Milli-Q system. Glass plates (Matsunami, S-1111, 3.8 cm × 1.3 cm × 0.1 cm) were treated overnight with a 1.0 mol dm^{-3} NaOH aqueous solution and washed thoroughly with water before use.

2.2. Preparation of CdS nanoparticles

MPTS-modified CdS nanoparticles were prepared by the procedure reported previously [48]. To each of 200 cm^3 of heptane solutions containing 14 g AOT and 5.7 cm^3 of water was added each of 1.3 cm^3 portions of a 1.0 mol dm^{-3} aqueous $Cd(ClO_4)_2$ solution and a 1.0 mol dm^{-3} aqueous Na_2S solution. After being stirred for 1 h, they were mixed together, resulting in the formation of CdS nanoparticles in AOT reversed micelles. To make the particle surfaces cadmium-rich, an additional 0.26 cm^3 portion of a 1.0 mol dm^{-3} aqueous $Cd(ClO_4)_2$ solution was added to the solution. The solution was stirred for another 1 h and then the solvent was removed by vacuum evaporation. To a toluene solution (400 cm^3) of the resulting yellow solid, a 5.0 cm^3 portion of 0.21 mol dm^{-3} MPTS toluene solution was added to modify the CdS surface, and then the solution was stirred for several hours.

2.3. Layer-by-layer accumulation of core–shell nanoparticles

Regulated accumulation of silica-coated CdS (core–shell) nanoparticles was conducted by repeated cycles of a procedure consisting of monoparticle layer deposition of the MPTS-modified CdS particles and hydrolysis of the remaining trimethoxysilyl groups to a silica network (Scheme 1a) as follows. Glass plates were treated with a refluxing toluene solution of the MPTS-modified CdS nanoparticles for 2 h, rinsed with methanol several times, and then heated in water at 363 K for 0.5 h. This deposition–hydrolysis cycle was repeated up to 17 times. Post-reaction curing was performed by heating for 1 h in an electric furnace under vacuum.

2.4. Size-selective photoetching of the CdS core

An argon-ion laser (Ion Laser Technology, model 5500A) and a 400 W mercury arc lamp (Eiko-sha) were used as light sources. The former was used for irradiation of monochromatic light at 488 and 458 nm. An emission line at 436 nm from the latter was extracted by the use of a combination of various types of glass optical filters. The silica-coated CdS nanoparticle films on a glass substrate were immersed in a 10 cm^3 oxygen-saturated aqueous solution of 50 μmol dm^{-3} MV^{2+} [47] and irradiated with monochromatic light until their absorption spectra had become unchanged. The absorption spectra of the silica-coated CdS nanoparticle films on glass plates were measured using an Agilent 8453 spectrophotometer. Since both sides of a glass plate were covered with nanoparticulate films, the absorption spectrum originating from a CdS film on one side, obtained by halving the absorbance, is shown in this paper.

2.5. Characterization of core–shell nanoparticle films

The surface of the film was observed by using an atomic force microscope (AFM) (Digital Instruments, Nanoscope IIIa) in a tapping mode using Nanosensors NCH cantilevers. The sizes of silica-coated CdS nanoparticles were determined by measuring the lateral dimension of the particle images (more than 60 particles).

3. Results and discussion

3.1. Layer-by-layer accumulation of nanoparticle films

An absorption spectrum of MPTS-modified CdS nanoparticles in toluene with an exciton peak around 445 nm and absorption onset at 530–550 nm is shown in Fig. 1a. Since the energy gap of bulk CdS has been reported to be 2.4 eV [49] (corresponding to the absorption onset of ca. 520 nm), most of the CdS nanoparticles possessed an energy gap similar to that of bulk material. As reported in a previous paper [48], CdS nanoparticles prepared by almost the same procedure had a wide size distribution ranging from 3 to 7 nm, with average diameter of 5.0 nm and standard deviation of 0.79 nm.

Before the addition of MPTS to the CdS particles in AOT reversed micelles, the surfaces of the particles were rich in cadmium. It is thought that the thiol group in MPTS (R–SH) reacts with these surface cadmium sites to make an R–S–Cd(CdS) linkage, i.e., the outermost surface layers of the particles are covered with trimethoxysilyl groups, which react strongly with hydroxyl groups on the glass substrate to give an Si(glass)–O–Si(MPTS) bond, as shown in Scheme 1a. Since no chemical reaction that results in

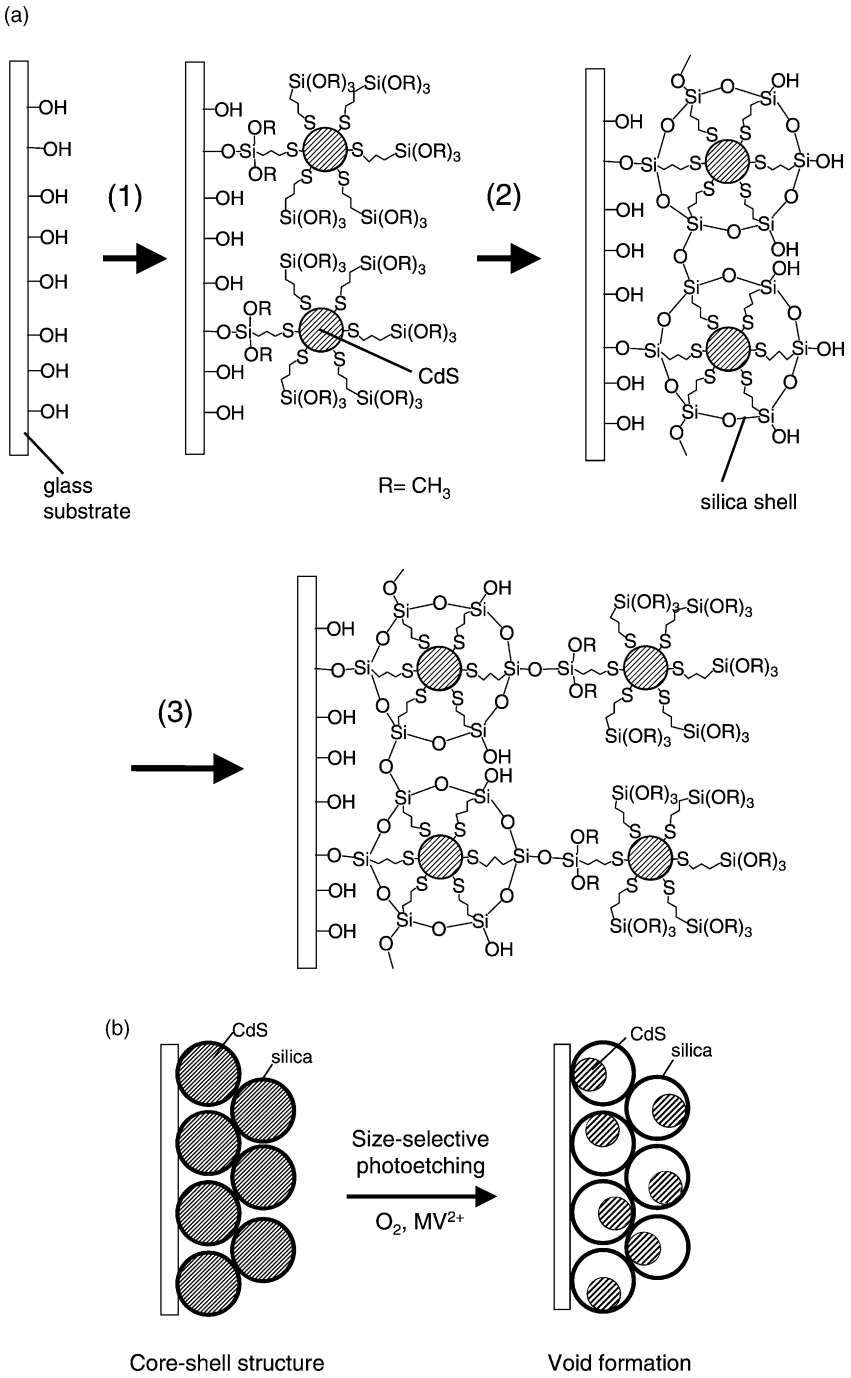

Scheme 1. (a) Preparation of a silica-coated CdS nanoparticle film by layer-by-layer deposition. Immobilization of MPTS-modified CdS nanoparticles (1, 3) and hydrolysis of trimethoxysilyl groups (2). (b) Regulation of void space inside the shell structure by size-selective photoetching.

binding of these particles is expected under dehydrated conditions as employed in the first deposition step, attachment of MPTS-modified CdS particles should be limited to coverage of, at most, a monoparticle layer; and no three-dimensional growth of the film should occur. The remaining trimethoxysilyl groups on anchored CdS nanoparticles are hydrolyzed in hot water to form a silica shell–CdS core structure, as was proved by FT-IR spectroscopy in our previous study [48]. Using the surface hydroxyl groups produced on the shell, another monoparticle layer of MPTS-modified CdS particles was attached, and this was followed by the hydrolysis. This layer-by-layer accumulation of silica-coated CdS was repeated up to 17 times.

Fig. 1b shows the absorption spectra of the silica-coated CdS nanoparticle films deposited on a glass plate. Although there was an upward shift of spectra in the whole wavelength range due to the light scattering of the films, the exciton peak of CdS nanoparticles could be detected at around 445 nm in

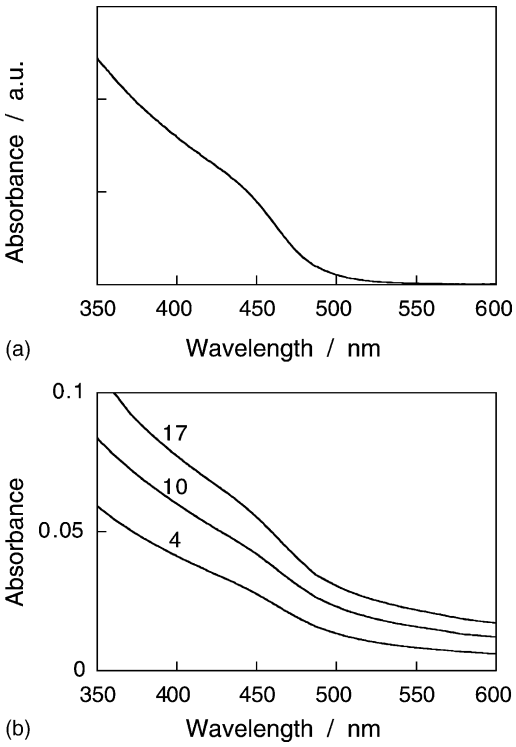

Fig. 1. (a) Absorption spectrum of MPTS-modified CdS nanoparticles dissolved in toluene. (b) Changes in the absorption spectra of silica-coated CdS nanoparticle films with an increase in the number of accumulation cycles. The number of accumulation cycles are indicated in the figure.

the spectra, in agreement with that of MPTS-modified CdS nanoparticles in solution, and its intensity was enhanced by increasing the number of accumulation cycles. Based on the assumption that the absorbance shift due to light scattering of the films is independent of wavelength, the absorbance (ΔA) owing to CdS was roughly estimated from the absorbance difference between the absorption onset (550 nm) and the exciton peak (445 nm). Fig. 2 shows ΔA as a function of the number of accumulation cycles. Average and standard deviation (error bar) values of 8–11 samples for each experiment, and are plotted in the figure. The relatively large error in ΔA measurement is due to different degree of light scattering at the peak wavelength. However, it is clear from the figure that there is a tendency for ΔA to increase with an increase in the number of repeated accumulations, and a linear line can be drawn as shown in the figure. From the slope of the linear relation, the number of the particles immobilized per cycle was estimated using the absorption coefficient of 536 $mol(CdS)^{-1}\,dm^3\,cm^{-1}$ at the exciton peak and the average diameter of CdS nanoparticles (5.0 nm) to be 2.1×10^{12} particles cm^{-2}. This value is 66% of that expected from a monoparticle layer of CdS nanoparticles (3.2×10^{12} particles cm^{-2}), the value of which was obtained by assuming two-dimensional hexagonal closed packing of silica-coated CdS nanoparticles consisting of a core of 5.0 nm in diameter and an MPTS overlayer of 0.5 nm in thickness. One possible reason for the loose packing is the

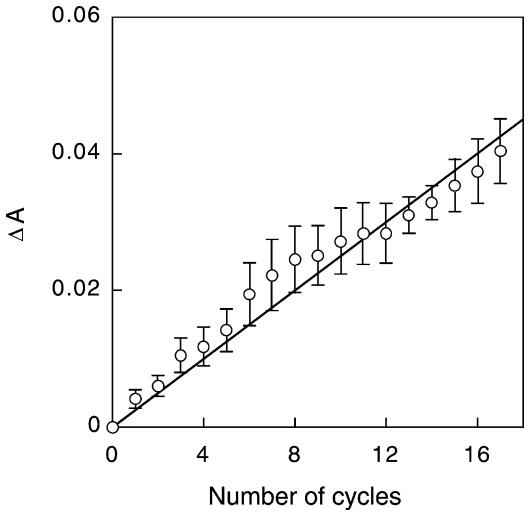

Fig. 2. Absorbance difference (ΔA) between exciton peak and absorption onset of silica-coated CdS nanoparticle films as a function of the number of accumulation cycles.

random deposition of nanoparticles as shown in AFM images (see below) due to heterogeneity of the size of CdS nanoparticles; the diameter of CdS core ranges from 3 to 7 nm [48].

3.2. Photoetching of the CdS core

Fig. 3 shows absorption spectra of the silica-coated CdS layers after irradiation of monochromatic light in water under aerated conditions. The absorption spectra of the resulting nanoparticles were blue-shifted and the exciton peak appeared more clearly along with a decrease in wavelength of irradiation light. It is well known that CdS

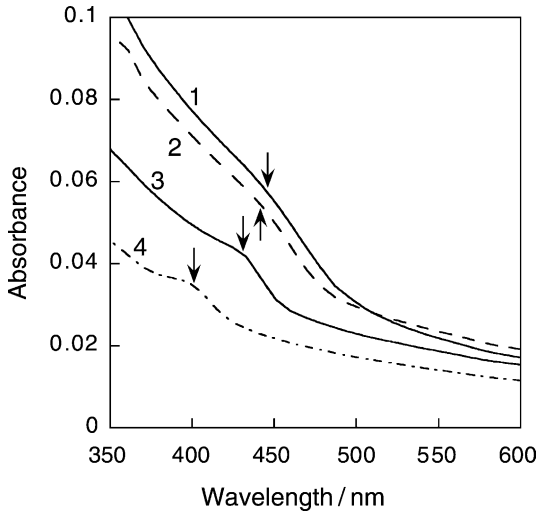

Fig. 3. Absorption spectra of silica-coated CdS nanoparticle films prepared by irradiation with various wavelengths: original film (1) and films prepared by irradiation at (2) 488 nm, (3) 458 nm, and (4) 436 nm. The number of accumulation cycles was 17. The arrows show the positions of exciton peaks.

particles become smaller due to photocorrosion (Eq. (1)) by irradiation under aerated conditions in the presence of an appropriate electron relay, such as MV^{2+} [42]:

$$CdS + 2O_2 \xrightarrow{h\nu} Cd^{2+} + SO_4{}^{2-} \quad (1)$$

The absorption onset of each spectrum seemed to agree with the wavelength of irradiation light. The fact suggested that the photocorrosion of CdS nanoparticles proceeded until the nanoparticles could not absorb light during the course of the photocorrosion, thus causing the absorption onset to shift a shorter wavelength due to an increase in the energy gap along with a decrease in the particle size, i.e., the size quantization effect. The exciton peak appeared at 440, 430, and 400 nm with monochromatic light irradiation at wavelengths of 488, 458, and 436 nm, respectively, from which diameters of photoetched CdS nanoparticles were estimated to be 3.3, 3.0, and 2.4 nm, respectively, by applying the experimentally obtained data to a theoretical relation between energy gap and particle diameter of CdS [50]. Thus, size-selective photoetching of silica-coated CdS nanoparticle films can be successfully performed, and the sizes of the resulting CdS nanoparticles can be adjusted by varying the wavelength of the monochromatic light, as reported in our previous paper [48]. The silica shells surrounding photoetched CdS nanoparticles might be porous enough for liberated Cd^{2+} and $SO_4{}^{2-}$ (Eq. (1)) to escape from the inside of the shell and at the same time prevent coalescence between the nanoparticles.

Fig. 4 shows the AFM images of silica-coated CdS nanoparticle films before and after irradiation at 458 nm. It was found that original silica-coated CdS nanoparticles were packed densely in the film and that the degree of the roughness of the film surface was relatively large (>50 nm). The average diameter of the original particles was determined to be 16 nm, with standard deviation of 7.4 nm, by measuring the lateral dimensions of particle images. When the surface of the film was measured after size-selective photoetching, similar morphology was observed, and the average diameter of particles was 15 nm with standard deviation of 5.3 nm, which were almost the same as the values obtained in original films. Considering that the uppermost layer, i.e., the silica shell of nanoparticles, was reflected in the AFM images, these results imply that monochromatic light irradiation did not induce shrinkage of the shell structure even when the size of the CdS core decreased with irradiation, resulting in the formation of a void space between the photoetched CdS core and the silica shell (Scheme 1b). Similar behavior has been observed in a study using TEM measurement of suspended silica-coated CdS nanoparticles, in which the size of the silica shell was almost equal to that of CdS nanoparticles before irradiation, regardless of the irradiation wavelength [48]. Although the diameters of the nanoparticles determined by AFM were much larger than those determined by TEM measurement, ca. 5.0 nm, it is well known that lateral size is often overestimated in AFM images because of the radius of the curvature of the point of AFM tips [51,52].

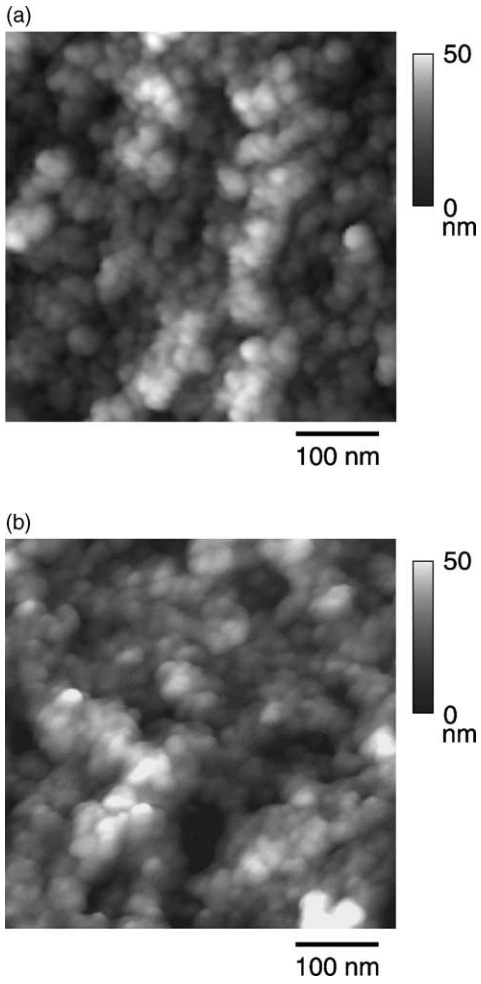

Fig. 4. AFM images of an original silica-coated CdS nanoparticle film (a) and that obtained with irradiation at 458 nm (b). The number of accumulation cycles was 17.

3.3. Effect of pre-irradiation curing

In order to increase the stability of the silica-coated CdS nanoparticle films, they were cured at various temperatures before photoetching. Fig. 5 shows the influence of curing temperature on absorption spectra before and after size-selective photoetching. Before photoetching, the absorption spectrum of the film heat-treated at 473 K was almost the same as that of the film without curing, but heat treatment at a temperature higher than 573 K caused an appreciable red-shift of absorption spectra, indicating that the sizes of deposited CdS nanoparticles had increased. In as-prepared nanoparticle films, a network of an Si–O–Si linkage surrounding the CdS particles is formed and separates the CdS particles. This silica network is connected to the CdS core particles through alkyl (C3) chain stems. When a part of the network surrounding one CdS particle is considered

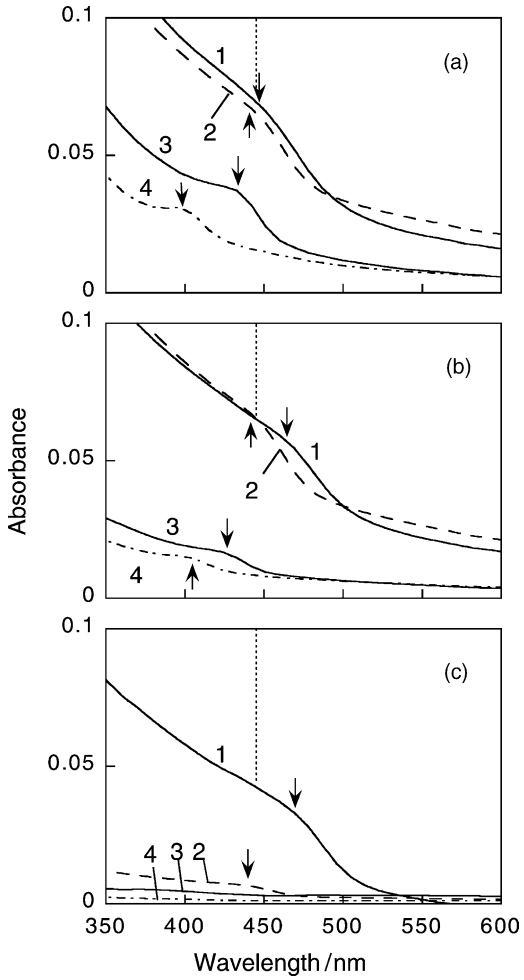

Fig. 5. Changes in the absorption spectra of silica-coated CdS nanoparticle films heat-treated at 473 K (a), 573 K (b), and 673 K (c) before (1) and after irradiation at (2) 488 nm, (3) 458 nm, and (4) 436 nm. The number of accumulation cycles was 17. The arrows show the positions of exciton peaks, and vertical dotted lines indicate the positions of exciton peaks of the as-prepared films.

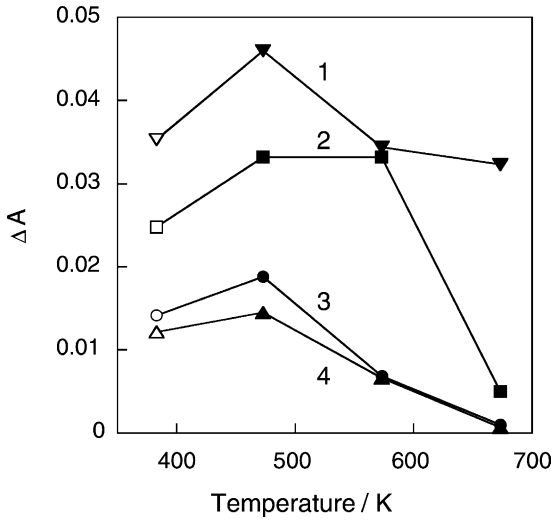

Fig. 6. Absorbance difference (ΔA) between exciton peak and absorption onset of silica-coated CdS nanoparticle films before (1) and after irradiation at (2) 488 nm, (3) 458 nm, and (4) 436 nm as a function of curing temperature. The results shown in Fig. 5 were used for calculation. The films were as-prepared (open symbols) and prepared after heat treatment (solid symbols).

as a chamber, the number of chambers in the whole film is equal to that of particles before curing. Heat treatment, especially that at a temperature higher than 573 K, might induce decomposition of the stems and appreciable shrinkage of the silica network, resulting in the formation of windows through the chambers. Growth of CdS particles by curing, as indicated by their spectral red-shift, is attributed to coalescence of CdS in neighboring chambers with the connecting window between them, the size of which is larger than that of the particle. The higher the temperature of curing is, the larger is the size of the window, i.e., the larger is the average size of CdS particles that might be formed after curing. Thermal acceleration of particle coalescence also accounts for the growth at a higher temperature. This view was supported by the results of AFM measurement of a nanoparticle film heat-treated at 673 K showing the average size and standard distribution of silica-coated CdS nanoparticles to be 19 and 8.5 nm, values larger than those obtained before heat-treatment (16 and 7.4 nm, respectively).

Size-selective photoetching was successfully performed regardless of the curing temperature as also shown in Fig. 5. The absorption spectra were blue-shifted and the absorption onset of each spectrum almost coincided with the irradiation wavelength. Furthermore, monochromatic light irradiation at 488, 458 and 436 nm gave exciton peaks at almost the same wavelength with or without curing (and regardless of curing temperature), except for the film cured at 673 K. It is noticeable that the absorbance, i.e., the amount of CdS after photoetching, decreased with an increase in curing temperature. Plots of the absorbance difference between exciton peak and absorption onset as a function of curing temperature are shown in Fig. 6, in which the data of an as-prepared film were plotted at the refluxing temperature, 383 K. At present we have no explanation for the increase in ΔA before irradiation at 473 K other than that the R–S–Cd moiety in the stem of the as-prepared film is converted to CdS via R–S-bond scission with negligible increase in particle size. This speculation is supported by the fact that absorbance changes of CdS nanoparticles were not observed during the process of the surface modification with MPTS and the expectation that sulfur atoms originally included in MPTS molecules will remain on CdS particles after curing. At a higher temperature, ΔA before irradiation decreased along with the red-shift of absorption spectra, i.e., growth of CdS particles, by the curing, probably due to the decrease in the molar absorption coefficient of the CdS unit with an increase in the diameters of CdS nanoparticles up to ca. 6 nm [53].

During the course of irradiation, CdS particles in chambers that are independent or connected through windows,

the sizes of which are smaller than those of the particles, undergo photoetching until their sizes become small enough for them to be able to pass through the window. This causes the coalescence of the photoetched CdS nanoparticles with each other to give larger particles, which are subjected to further photocorrosion. This implies that the photocorrosion continues unless the total number of remaining particles becomes so small that they cannot coalesce. Similar values of ΔA for original and 488 nm photoetched samples at curing temperature between 473 and 573 K suggest that the average size of windows formed in this temperature range is smaller than the sizes of original particles or those of nanoparticles photoetched at 488 nm irradiation. On the other hand, this window size might be large enough for the coalescence of particles photoetched at 458 or 436 nm irradiation, resulting in the marked decrease in ΔA. The behavior of ΔA for films cured at 673 K can be explained similarly. On the basis of these results, it is thought that the silica shell of the core–shell nanoparticles is stabilized by alkyl chain stems anchored to the CdS core surface but shrinks due to the removal of stems by curing, leading to the formation of windows connecting the chambers and allowing the coalescence of photoetched particles.

4. Conclusion

We have successfully immobilized silica-coated CdS core–shell nanoparticles on glass substrates using a newly developed layer-by-layer accumulation technique. Spectroscopic analyses revealed that the packing density of nanoparticles is less than that of hexagonal close packing of particles of uniform size. This was attributed to the heterogeneity of actual particle size, which interferes with the close packing. In the next step of our study, we will try to accumulate the layers of nanoparticles which were monodispersed by using size-selective photoetching. As expected, size-selective photoetching of nanoparticle films results in a decrease in the size of the CdS core depending on the wavelength of irradiation light, while the shell structures of the immobilized nanoparticles were almost unchanged, indicating that void spaces are created between the photoetched core and the silica shell and that their sizes can be regulated by choosing the irradiation wavelength. Nanospaces of regulated size in photoetched particulate films containing semiconducting materials of uniform size (i.e., of uniform chemical and physical properties) can be as a new type of reaction spaces, e.g., a nanoflask array for semiconductor photocatalytic reactions. It was revealed, in contrast to our expectation, that curing of the film induced shrinkage of the silica network of shells, resulting in a decrease in the number of remaining photoetched CdS cores. In order to avoid this, it is necessary, for example, to fill the gaps among core–shell particles or thicken the silica shell layer. Work in this direction is currently in progress.

References

[1] P. Mulvaney, L.M. Liz-Marzan, M. Giersig, T. Ung, J. Mater. Chem. 10 (2000) 1259.
[2] R.A. Caruso, M. Antonietti, Chem. Mater. 13 (2001) 3272.
[3] F. Caruso, Adv. Mater. 13 (2001) 11.
[4] E. Bourgeat-Lami, J. Nanosci. Nanotechnol. 2 (2002) 1.
[5] L.M. Liz-Marzan, M. Giersig, P. Mulvaney, Langmuir 12 (1996) 4329.
[6] A.R. Kortan, R. Hull, R.L. Opila, M.G. Bawendi, M.L. Steigerwald, P.J. Carroll, L.E. Brus, J. Am. Chem. Soc. 112 (1990) 1327.
[7] B.O. Dabbousi, J. RodriguezViejo, F.V. Mikulec, J.R. Heine, H. Mattoussi, R. Ober, K.F. Jensen, M.G. Bawendi, J. Phys. Chem. B 101 (1997) 9463.
[8] A. Mews, A. Eychmueller, M. Giersig, D. Schooss, H. Weller, J. Phys. Chem. 98 (1994) 934.
[9] M.T. Harrison, S.V. Kershaw, A.L. Rogach, A. Kornowski, A. Eychmuller, H. Weller, Adv. Mater. 12 (2000) 123.
[10] I. Bedja, P.V. Kamat, J. Phys. Chem. 99 (1995) 9182.
[11] P.V. Kamat, B. Shanghavi, J. Phys. Chem. B 101 (1997) 7675.
[12] M. Bruchez Jr., M. Moronne, P. Gin, S. Weiss, A.P. Alivisatos, Science 281 (1998) 2013.
[13] D. Gerion, F. Pinaud, S.C. Williams, W.J. Parak, D. Zanchet, S. Weiss, A.P. Alivisatos, J. Phys. Chem. B 105 (2001) 8861.
[14] S.Y. Chang, L. Liu, S.A. Asher, J. Am. Chem. Soc. 116 (1994) 6739.
[15] T. Ung, L.M. Liz-Marzan, P. Mulvaney, J. Phys. Chem. B 105 (2001) 3441.
[16] F. Garcia-Santamaria, V. Salgueirino-Maceira, C. Lopez, L.M. Liz-Marzan, Langmuir 18 (2002) 4519.
[17] M. Hara, J.T. Lean, T.E. Mallouk, Chem. Mater. 13 (2001) 4668.
[18] S.W. Keller, S.A. Johnson, E.S. Brigham, E.H. Yonemoto, T.E. Mallouk, J. Am. Chem. Soc. 117 (1995) 12879.
[19] S.W. Kim, M. Kim, W.Y. Lee, T. Hyeon, J. Am. Chem. Soc. 124 (2002) 7642.
[20] K. Dick, T. Dhanasekaran, Z.Y. Zhang, D. Meisel, J. Am. Chem. Soc. 124 (2002) 2312.
[21] E. Hutter, J.H. Fendler, Chem. Commun. (2002) 378.
[22] S.Y. Chang, L. Liu, S.A. Asher, J. Am. Chem. Soc. 116 (1994) 6745.
[23] R.A. Caruso, A. Susha, F. Caruso, Chem. Mater. 13 (2001) 400.
[24] F. Caruso, M. Spasova, A. Susha, M. Giersig, R.A. Caruso, Chem. Mater. 13 (2001) 109.
[25] L. Sun, R.M. Crooks, V. Chechik, Chem. Commun. (2001) 359.
[26] K.P. Velikov, A. van Blaaderen, Langmuir 17 (2001) 4779.
[27] O.V. Makarova, A.E. Ostafin, H. Miyoshi, J.R. Norris, D. Meisel, J. Phys. Chem. B 103 (1999) 9080.
[28] S.M. Marinakos, J.P. Novak, L.C. Brousseau, A.B. House, E.M. Edeki, J.C. Feldhaus, D.L. Feldheim, J. Am. Chem. Soc. 121 (1999) 8518.
[29] S.M. Marinakos, M.F. Anderson, J.A. Ryan, L.D. Martin, D.L. Feldheim, J. Phys. Chem. B 105 (2001) 8872.
[30] S.O. Obare, N.R. Jana, C.J. Murphy, Nano Lett. 1 (2001) 601.
[31] B. Rodriguez-Gonzalez, V. Salgueirino-Maceira, F. Garcia-Santamaria, L.M. Liz-Marzan, Nano Lett. 2 (2002) 471.
[32] Y. Yin, Y. Lu, B. Gates, Y. Xia, Chem. Mater. 13 (2001) 1146.
[33] Y.G. Sun, B.T. Mayers, Y.N. Xia, Nano Lett. 2 (2002) 481.
[34] Y.G. Sun, Y.N. Xia, Anal. Chem. 74 (2002) 5297.
[35] M. Giersig, T. Ung, L.M. Liz-Marzan, P. Mulvaney, Adv. Mater. 9 (1997) 570.
[36] M. Giersig, L.M. Liz-Marzan, T. Ung, D.S. Su, P. Mulvaney, Ber. Bunsen-Ges. Phys. Chem. 101 (1997) 1617.
[37] M. Kim, K. Sohn, H.B. Na, T. Hyeon, Nano Lett. 2 (2002) 1383.
[38] S.T. Yau, P. Mulvaney, W. Xu, G.M. Spinks, Phys. Rev. B 57 (1998) R15124.
[39] F.G. Aliev, M.A. Correa-Duarte, A. Mamedov, J.W. Ostrander, M. Giersig, L.M. Liz-Marzan, N.A. Kotov, Adv. Mater. 11 (1999) 1006.
[40] I. Pastoriza-Santos, D.S. Koktysh, A.A. Mamedov, M. Giersig, N.A. Kotov, L.M. Liz-Marzan, Langmuir 16 (2000) 2731.

[41] D.S. Koktysh, X.R. Liang, B.G. Yun, I. Pastoriza-Santos, R.L. Matts, M. Giersig, C. Serra-Rodriguez, L.M. Liz-Marzan, N.A. Kotov, Adv. Funct. Mater. 12 (2002) 255.
[42] H. Matsumoto, T. Sakata, H. Mori, H. Yoneyama, J. Phys. Chem. 100 (1996) 13781.
[43] T. Torimoto, H. Nishiyama, T. Sakata, H. Mori, H. Yoneyama, J. Electrochem. Soc. 145 (1998) 1964.
[44] M. Miyake, T. Torimoto, T. Sakata, H. Mori, H. Yoneyama, Langmuir 15 (1999) 1503.
[45] T. Torimoto, H. Kontani, T. Sakata, H. Mori, H. Yoneyama, Chem. Lett. (1999) 379.
[46] T. Torimoto, N. Tsumura, H. Nakamura, S. Kuwabata, T. Sakata, H. Mori, H. Yoneyama, Electrochim. Acta 45 (2000) 3269.
[47] T. Torimoto, H. Kontani, Y. Shibutani, S. Kuwabata, T. Sakata, H. Mori, H. Yoneyama, J. Phys. Chem. B 105 (2001) 6838.
[48] T. Torimoto, J.P. Reyes, K. Iwasaki, B. Pal, T. Shibayama, K. Sugawara, H. Takahashi, B. Ohtani, J. Am. Chem. Soc. 125 (2003) 316.
[49] Y.V. Pleskov, Y.Y. Gurevich, Semiconductor Photoelectrochemistry Consultants Bureau, New York, 1986.
[50] P.E. Lippens, M. Lannoo, Phys. Rev. B 39 (1989) 10935.
[51] L. Sun, M. Crooks, Langmuir 18 (2002) 8231.
[52] T. Sagara, N. Kato, N. Nakashima, J. Phys. Chem. B 106 (2002) 1205.
[53] T. Vossmeyer, L. Katsikas, M. Giersig, I.G. Popovic, K. Diesner, A. Chemseddine, A. Eychmueller, H. Weller, J. Phys. Chem. 98 (1994) 7665.